Structure-Preserving Model Reduction of Nonlinear Building Thermal Models ⋆

Kun Deng [a], Siddharth Goyal [b], Prabir Barooah [b], Prashant G. Mehta [a]

[a] *Coordinated Science Laboratory, University of Illinois at Urbana-Champaign, Urbana, IL 61801, USA*

[b] *Department of Mechanical and Aerospace Engineering, University of Florida, Gainesville, FL 32611, USA*

Abstract

This paper proposes an aggregation-based model reduction method for nonlinear models of multi-zone building thermal dynamics. The full-order model, which is already a lumped-parameter approximation, quickly grows in state space dimension as the number of zones increases. An advantage of the proposed method, apart from being applicable to the nonlinear thermal models, is that the reduced model obtained has the same structure and physical intuition as the original model. The key to the methodology is an analogy between a continuous-time Markov chain and the linear part of the thermal dynamics. A recently developed aggregation-based method of Markov chains is employed to aggregate the large state space of the full-order model into a smaller one. Simulations are provided to illustrate tradeoffs between modeling error and computation time.

Key words: Model reduction; Structure preserving; Model-based control; Numerical simulation; Markov models.

1 Introduction

A typical building HVAC (Heating, Ventilation, and Air Conditioning) system consists of AHUs, supply ducts, and terminal boxes; see Fig. 1. The AHU (Air Handling Unit) supplies conditioned air to terminal boxes at so-called leaving-air temperature and humidity. Each terminal box delivers air to one or more zones. Using reheat coil, the supply air temperature can be increased beyond the AHU leaving temperature. In a VAV (Variable-Air-Volume) system, the terminal box can vary the supply air mass flow rate through dampers. A controller at each terminal box can be used to maintain the temperature of a zone at a specified value by controlling the mass flow rate of air supplied to the zone.

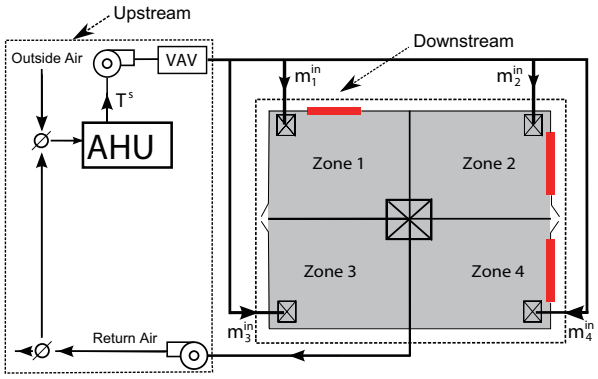

Fig. 1. The configuration of a four-zone building HVAC system.

For a building HVAC system, conventional controls include rule-based controls and single-loop PID controls that are simple and normally work with single objective, e.g. reference tracking, offset prevention, etc. But these controls are known not to be optimal in either thermal comfort or energy consumption for building HVAC systems [11,20,24]. In contrast to conventional controls, modern controls of a building HVAC system are typically fulfilled using a two-level control structure: a supervisory level and a local level [24]. The goal of the supervisory-level control is to optimize the operations of building systems for minimizing energy consumption while satisfying human thermal comfort. Well-developed supervisor controls can improve the energy efficiency and adapt to the changing environment. The local-level control modulates the individual devices (e.g. a re-

⋆ The material in this paper was partially presented at the American Control Conference on June 30-July 2, 2010, Baltimore, MA, USA. The research is supported by the National Science Foundation under Grants CNS-0931416, CNS-0931885, and ECCS-0955023. Corresponding author Kun Deng. Tel. +1 217 390 9567. Fax +1 217 244 4333.

Email addresses: kundeng2@illinois.edu (Kun Deng), siddgoya@ufl.edu (Siddharth Goyal), pbarooah@ufl.edu (Prabir Barooah), mehtapg@illinois.edu (Prashant G. Mehta).

lay, an actuator, etc.) to track the set-points provided by the supervisory-level control. A closed-loop feedback control (e.g. PID control) is usually used to achieve the set-point tracking performance. Well-tuned local-loop controllers can enhance the space thermal comfort, reduce energy use, and extend the component life. The overall energy efficiency and control effectiveness of the building HVAC system is determined by the performance and coordination of controls in both levels.

Utilization of physical models in supervisory-level control can largely minimize building-wide energy consumption and properly satisfy thermal comfort requirements [11]. The performance of model-based controls highly relies on the models that are used to describe the thermal behavior of building zone temperatures and capture the energy consumption of building operations. In this paper, we capture the building thermal dynamics using energy and mass balance equations. A thermal resistor-capacitor (RC) network model is established to represent thermal dynamics of a multi-zone building with nodes representing zones or internal surface points. This model can be used for many purposes in building controls. For example, the models can be used for off-line simulations that advise the system operators with the best operating strategy, e.g. simulation-assisted control [24]. The models can also be used for on-line optimizations and controls that determine optimal operating set-points for local feedback controllers, e.g. Model Predictive Control (MPC) [15, 20, 25]. Besides enabling advanced controls, the models can also provide useful capabilities for performance analysis [9] and system identification [3].

Model reduction techniques of building thermal models are essentially important for many practical estimation and control applications. First, it is worth noting that there are computer aided building modeling tools that result in complex RC-network models similar to the one presented in this paper, e.g., EnergyPlus [10] and TRNSYS [18]. These complex building models could be used for off-line computer simulations to accurately predict building temperature evolution and energy consumption. But the complexity of these models grows exponentially as the number of building zones increases [9, 13, 14]. A large amount of measurement data is required to identify the parameters used for these complex models, which usually causes data over-fitting problems and high modeling uncertainties [10]. Thus it is necessary to consider the reduced models with simpler structure and less number of parameters for the ease of parameter estimation and data fitting. Second, the model complexity is a major issue for implementing the online optimization-based control schemes, e.g. MPC, particularly if the optimization is to be performed with a day-long prediction horizon to take advantage of slow thermal responses of buildings as well as daily variations in environment and energy prices [20, 25]. The complexity and accuracy of models both play important roles for the success of MPC. It is essential to develop reduced models to achieve a trade-off between prediction accuracy and model complexity. The focus of this paper is on model reduction of multi-zone building thermal dynamics.

The building thermal model presented here is a nonlinear model with a linear term capturing the nodal thermal interactions and a bilinear term due to the heat flux into the zone space. Due to the nonlinear nature of the model, the number of available techniques for model reduction is limited. Balanced truncation methods for nonlinear systems use controllability and observability energy functions of a system to find the reduced realizations [17, 22]. Lall *et al.* in [19] use empirical Gramians to determine the importance of a particular subspace in terms of its contribution to the input-output behavior. These energy functions or empirical Gramians however are difficult to compute in practice [14]. Moreover, the reduced models generated by truncation methods do not retain the physical intuition of the full model, i.e., truncated states of the reduced model usually have no physical meanings.

In this paper, we propose an *aggregation-based* model reduction method that preserves the RC-network structure of the nonlinear building thermal model. This is achieved by obtaining super-nodes via aggregation of building nodes. The aggregation-based approach proposed in this paper is based on model reduction method of Markov chains that has recently been developed in [8]. The main idea here is to connect the linear part of building thermal model to a continuous-time Markov chain, and apply the aggregation method of Markov chains to systematically find optimal coordination of aggregation and the optimal linear dynamics. The nonlinear model part is then aggregated accordingly based on the same optimal coordination. The major advantage of the proposed aggregation-based method compared to truncation-based methods is the *structure-preserving* property in the sense that the reduced model is still a RC-network with parameters and nodes maintaining the same physical meaning as the full building model. The other advantage is that it does not suffer from the computational difficulties of empirical Gramians or energy functions.

For practical control applications, a linear model could be obtained by linearizing the nonlinear model around operating points. Then the linearized model can be used for designing linear quadratic regulator, Kalman filter, and linear model predictive control, etc. If the actual operation points move away from the vicinity of system linearization point, the performance of the linearized model will be degraded and a running linearization is needed to ensure the control performance [21]. Besides considering linearzied models, the direct utilization of nonlinear models such as the full and reduced models presented in this paper could also be beneficial for the building HVAC community. Interests in nonlinear optimization techniques with nonlinear building models have been on the increase in recent years [11]. Some novel control methods are also proposed by exploring the specific structure of the nonlinear building thermal model. In [24], a Hammerstein-Wiener nonlinear MPC is proposed and studied, where the original nonlinearities included in a building thermal dynamics are handled through nonlinear static mappings. In [5], a decentralized optimal control strategies is proposed to improve the building energy efficiency, where

the reduced models developed in this paper is used to capture the net effect of the entire building envelope on any individual zone.

The method proposed in this paper is an extension of its conference version [6], where we only apply the aggregation method to a linear building thermal model. This paper extends the aggregation method to a more realistic nonlinear building thermal model, and assesses the performance and computational complexity of reduced-order models through numerical simulations. The aggregation-based method proposed here are related to model reduction techniques for grey-box models [4], where the model structure and parameters are obtained through the physical insights. The aggregated building model can be thought as a grey-box model and coordination of aggregation specifies the model structure. The aggregation-based method described here can also be used to creates zoning approximations for building models by combining zones together. In a very recent work [12], a Koopman operator approach is proposed to systematically create zoning approximation for buildings, where the dominant modes of thermal behavior are extracted from the building simulations. Then modes information is used to combine multiple zones into single zones. The major difference is that our method is directly based on the knowledge of building descriptions, while the method in [12] is mainly based on data from building simulations.

2 Full-order Building Thermal Model

The focus of this paper is on model reduction of the building zone thermal dynamics, which suffer more of modeling complexity than the AHU dynamics [6]. As a result, the AHU dynamics are replaced by static gains in this paper without significant loss of accuracy. A lumped parameter model of resistances and capacitances is constructed to describe the thermal dynamics of a multi-zone building, with current and voltage being analogous to heat flow and temperature, respectively. We only consider the interzone conductive heat transfer but ignore the convective heat transfer that occurs through the open windows, doors, and hallways. The 3R2C models of surface elements (e.g., walls, windows, ceilings, and floors) are inter-connected to construct a RC-network model for building thermal dynamics [13]. The set $\mathcal{V} := \{1, \ldots, n+1\}$ denotes the set of nodes of the network. The nodes are assumed to be re-indexed so that the first N nodes correspond to $1, \ldots, N$ physical zones, and the next $(n-N)$ nodes correspond to the points internal to the surfaces that appear due to the 3R2C models. The last $(n+1)$th node corresponds to the outside.

For each node $i \in \mathcal{V}$, the associated temperature and thermal capacitance are denoted as T_i and C_i, respectively. Let $\mathcal{E}$ denote the set of all edges of the RC-network, where edges represent pathways for conductive heat transports. For any nodes $i, j \in \mathcal{E}$, the thermal resistance between i and j is represented as a lumped parameter R_{ij}, with $R_{ji} = R_{ij}$ by convention. The inputs to the building model are summarized here: $\dot{m}_i^{in}$ denotes the mass flow rate of the supply air, $\dot{Q}_i^r$ denotes the heat gain due to reheating that may occur at the VAV box, $\dot{Q}_i^{int}$ denotes the internal heat gain (i.e., the rate of heat generated by occupants, equipments, lights, etc.), and $\dot{Q}_i^{ext}$ denotes the external heat gain (i.e., the rate of solar radiation). It is assumed that (i) the values of C_i and R_{ij} are known parameters obtained based on building structures and materials, (ii) the supply air temperature T^s is assumed to be a constant here, and (iii) the (estimation of) the outside temperature T_o and the heat gains $\dot{Q}^r, \dot{Q}^{int}, \dot{Q}^{ext}$ are available based on historical data, weather forecast, and sensor measurements.

A good estimate of the major parameters (e.g. thermal resistance, thermal conductivity, heat exchange coefficient, etc.) is very important for the effectiveness of the building thermal model. These parameters can be either extracted from a well-established building information model (BIM) or from a data-driven system identification process. In the first approach, the goodness of the estimated parameters can be validated by comparing the simulation of the building thermal model with an EnergyPlus simulation of the BIM [9]. In the second approach, a (wireless) sensor network can be used to collect the measurement data of indoor space temperature, ambient temperature, occupancy information, supplied air mass flow rate, and electricity usage [3]. Then system identification techniques can be employed to estimate parameters using the building thermal model and the measured data. In this paper, we assume all parameters used in the model have already been well estimated using aforementioned methods.

In the following, a compact state-space representation is presented for building thermal dynamics. To establish a Markov chain analogy in the next section, the outside temperature is also taken as a "virtual state" T_{n+1} to the building system. We assign a very large "virtual capacitance" to the outside node: $C_{n+1} \gg C_i$, for $i = 1, \ldots, n$. Letting $C_{n+1} \to \infty$, the dynamic equations are derived from the energy balance laws:

$$\frac{dT}{dt} = AT + L(T, U, \dot{Q}) \tag{1}$$

where the state vector $T := [T_1, \ldots, T_{n+1}]^T$, the control vector $U := [\dot{m}_1^{in}, \ldots, \dot{m}_N^{in}, 0, \ldots, 0]^T$, and the heat gain vector $\dot{Q} := [\dot{Q}_1, \ldots, \dot{Q}_N, 0, \ldots, 0]^T$.

- The transition rate matrix A is a $(n+1) \times (n+1)$ matrix is given by

$$A_{ij} = \begin{cases} 0, & \text{if } j \neq i,\ (i,j) \notin \mathcal{E} \\ 1/(C_i R_{ij}), & \text{if } j \neq i,\ (i,j) \in \mathcal{E} \\ -\sum_{k \neq i} A_{ik}, & \text{if } j = i,\ (i,j) \in \mathcal{E} \end{cases} \tag{2}$$

- The nonlinear function is given by

$$\begin{cases} L_i(T,U,\dot{Q}) = \dfrac{C_{pa}U_i(T^s - T_i) + \dot{Q}_i}{C_i}, & i = 1,\ldots,N \\ L_i(T,U,\dot{Q}) = 0, & i = N+1,\ldots,n \\ L_i(T,U,\dot{Q}) = \eta, & i = n+1 \end{cases}$$

where C_{pa} is the specific heat capacitance of the supply air and $\dot{Q}_i$ is the total heat gains from all sources

$$\dot{Q}_i(t) = \dot{Q}_i^r(t) + \dot{Q}_i^{int}(t) + \dot{Q}_i^{ext}(t).$$

The function $\eta(t) \in \mathbb{R}$ is chosen such that $\eta(t) = \dot{T}_o(t)$, the derivative of the outside temperature. Note that the entries in the last row of A approach 0 as $C_{n+1} \to \infty$ (since they are of the form $1/(C_{n+1}R_{n+1,j})$). In the limit, $\dot{T}_{n+1} = \eta(t)$, which gives $T_{n+1}(t) = T_o(t)$ for all $t \geq 0$.

Remark 1 Note that the linear term AT in (1) captures the thermal interactions of neighboring nodes. The nonlinear term $L(T,U,\dot{Q})$ in (1) can be interpreted as a current source injected into the RC-network, except that the source strength depends on the "voltage" T. Thus, the building thermal model can be thought as a RC-network model with additional current sources, where the source strengths depend on the voltage of nodes they are connected to.

3 Reduced-order Building Thermal Model

3.1 Markov chain analogy to linear dynamics

In this section, we show that the linear part of the building thermal model (1), given below

$$\frac{dT}{dt} = AT \tag{3}$$

is analogous to a *continuous-time Markov chain*. This analogy will be used later in this paper to obtain the optimal aggregation of the state space through a recently developed Markov chain aggregation method [8].

Consider a scalar-valued function $V(t) := \sum_{i\in\mathcal{V}} C_iT_i(t)$. As shown in [6], $V(t)$ is an invariant quantity, i.e., $V(t) = V(0)$ for all $t \geq 0$ due to the fact that the matrix A is a intensity matrix, i.e., every row sum is equal to zero, all diagonal entries are negative, and all non-diagonal entries are non-negative (see (2)). Define a row vector f with $f_i = C_iT_i/V(0)$ for $i \in \mathcal{V}$. Then, one can verify that

- The vector f is a probability distribution vector, i.e., $\sum_{i\in\mathcal{V}} f_i(t) \equiv 1$ for all $t \geq 0$.
- The vector f satisfies the following dynamic equation

$$\frac{df}{dt} = fA \qquad \Rightarrow \qquad f(t) = f(0)e^{At}.$$

Due to the special structure of the matrix A, the set $\{P(t) := e^{At}\}_{t\geq 0}$ forms a *transition semigroup*: For any $t, s \geq 0$, (i) $P(0) = I$, (ii) $P(t)$ is a stochastic matrix, and (iii) $P(t+s) = P(t)P(s)$. Consider a continuous-time Markov chain $\{X(t)\}_{t\geq 0}$ on the state space $\mathcal{V}$ with the transition semigroup $\{P(t)\}_{t\geq 0}$ [23]. Let $g(t)$ denote its probability distribution at time t, i.e., $g_i(t) = \text{Prob}(X(t) = i)$ for any $i \in \mathcal{V}$. If we take $f(0)$ as the initial distribution of $\{X(t)\}_{t\geq 0}$, then

$$g(t) = g(0)P(t) = f(0)e^{At} = f(t).$$

The Markov chain analogy is now clear. Starting from the same initial distribution, the probability distribution of the continuous-time Markov chain $\{X(t)\}_{t\geq 0}$ is equal to the thermal distribution of the linear thermal model (3).

For any ergodic Markov chain, there exists a unique *stationary distribution* π (obtained as a solution to $\pi A = 0$), whereby starting from any initial distribution, $\lim_{t\to\infty} g(t) = \pi$. For linear thermal model (3), the associated Markov chain is shown to be ergodic in [6], and the stationary distribution is given by:

$$\pi_i = \frac{C_i}{\sum_{j\in\mathcal{V}} C_j}, \quad i \in \mathcal{V}. \tag{4}$$

The notation (π, P) is used to denote a Markov chain with the transition matrix P and the stationary distribution π. For more details on continuous-time Markov chains, we refer the reader to [23] and references therein.

3.2 Model reduction via aggregation

An aggregation methodology is considered in this paper for the model reduction purpose: Mathematically, suppose the goal is to reduce the state space dimension from n to m, where $m \leq n$ is a (user-specified) number of super-nodes or degree of reduction. The coordinate information of aggregation is defined by a *partition function* $\phi : \mathcal{V} \to \bar{\mathcal{V}}$, where $\bar{\mathcal{V}} = \{1,\ldots,m+1\}$ denotes the set of "super-nodes" for the reduced-order model, and recall that $\mathcal{V} = \{1,\ldots,n+1\}$ denotes the set of nodes for the full-order model. A partition function is an onto function but possibly many-to-one. The elements of $\bar{\mathcal{V}}$ are the super-nodes, and for every $k \in \bar{\mathcal{V}}$, the inverse mapping $\phi^{-1}(k) \subset \mathcal{V}$ denotes the group of nodes in the full-order model that are aggregated into the kth super-node using the partition function ϕ.

For each super-node $k \in \bar{\mathcal{V}}$, we introduce a super-temperature $\bar{T}_k$, a super-capacitance $\bar{C}_k$, and a super-resistance $\bar{R}_{kl}$. For a given ϕ, the reduced-order model for (3) has the form:

$$\frac{d\bar{T}}{dt} = \bar{A}(\phi)\bar{T}, \tag{5}$$

where $\bar{T} = [\bar{T}_1,\ldots,\bar{T}_{m+1}]^T$ denotes the super-temperature vector, and $\bar{A}(\phi)$ denotes the $(m+1)\times(m+1)$ super-transition-rate matrix. The Markov chain analogy also works

for the reduced-order model (5) with the associated transition semigroup $\{\bar{P}(t) := e^{\bar{A}(\phi)t}\}_{t\geq 0}$.

Recall that the outside node is a virtual $(n+1)$th node in $\mathcal{V}$. We also take the outside node as a virtual $(m+1)$th node in $\bar{\mathcal{V}}$. Thus, we are interested in those partition functions such that the building node set $\{1,\ldots,n\}$ is partitioned into the super-node set $\{1,\ldots,m\}$, and the $(n+1)$th outside node has a one-to-one correspondence to the $(m+1)$th super-node. In this paper, the optimal partition function is chosen through the Markov aggregation method described below.

3.3 Optimal aggregation of Markov chain

In this section, we summarize our recently developed Markov aggregation method [8]. Consider two Markov chains (π, P) and $(\bar{\pi}, \bar{P})$ defined on two different state spaces $\mathcal{V}$ and $\bar{\mathcal{V}}$, respectively. To compare two chains on the same state space $\mathcal{V}$, we apply the lifting technique by defining the π-lifting transition matrix of $(\bar{\pi}, \bar{P})$ as:

$$\widehat{P}^{(\pi)}_{ij}(\phi) = \frac{\pi_j}{\sum_{k\in\psi(j)}\pi_k} P_{\phi(i)\phi(j)}, \quad i,j \in \mathcal{V} \qquad (6)$$

where $\psi(j) = \phi^{-1}\circ\phi(j)$ denotes the set of states belonging to the same group as the jth state. The Kullback-Leibler (KL) divergence rate is employed as a "probability distance" to quantify the differences between (π, P) and $(\bar{\pi}, \bar{P})$:

$$R_\phi(P\|\bar{P})) = \sum_{i,j\in\mathcal{V}} \pi_i P_{ij} \log\left(P_{ij}/\widehat{P}^{(\pi)}_{ij}(\phi)\right).$$

The optimal aggregation problem is given below:

$$\begin{aligned} &\min_{\phi,\bar{P}} \; R_\phi(P\|\bar{P}) \\ &\text{s.t.} \quad \bar{P}\mathbf{1} = \mathbf{1},\ \bar{P} \geq 0. \end{aligned}$$

As shown in Theorem 2 of [8], for a fixed (whether optimal or not) partition function ϕ, the optimal aggregated Markov chain $(\bar{\pi}(\phi), \bar{P}(\phi))$ has the form:

$$\bar{P}_{kl}(\phi) = \frac{\sum_{i\in\phi^{-1}(k)}\sum_{j\in\phi^{-1}(l)}\pi_i P_{ij}}{\sum_{i\in\phi^{-1}(k)}\pi_i}, \quad k,l\in\bar{\mathcal{V}} \qquad (7)$$

where the stationary distribution of $\bar{P}(\phi)$ is given by

$$\bar{\pi}_k(\phi) = \sum_{i\in\phi^{-1}(k)} \pi_i, \quad k\in\bar{\mathcal{V}}. \qquad (8)$$

As a result, the optimal aggregation problem reduces to finding only an *optimal partition function* $\phi^* : \mathcal{V}\to\bar{\mathcal{V}}$ such that

$$\phi^* \in \arg\min_{\phi} \; R_\phi(P\|\bar{P}(\phi)). \qquad (9)$$

It is shown in [8] that solving the optimization problem (9) exactly is difficult when degree of reduction $m \geq 2$. Instead, a heuristic spectral partitioning algorithm is proposed to obtain a suboptimal solution of (9): For the bi-partition problem, ϕ^* is obtained using the sign-structure of the second eigenvector of the symmetric matrix $\widetilde{P} = \frac{1}{2}(\Pi^{\frac{1}{2}}P\Pi^{-\frac{1}{2}} + \Pi^{-\frac{1}{2}}P^T\Pi^{\frac{1}{2}})$, where $\Pi = \mathrm{diag}(\pi)$. The sub-optimal solution of the multi-partition problem is obtained via recursive application of the bi-partition algorithm.

3.4 Optimal reduced linear dynamics

In this section, we apply the Markov aggregation method to obtain the optimal reduced linear thermal model. Discretizing the system with a small step-size Δt, we consider the Markov transition matrices $P(\Delta t)$ and $\bar{P}(\Delta t)$ associated with the full and reduced building models, respectively. We can approximately express $P(\Delta t) = I + A\Delta t + O(\Delta t^2)$ and $\bar{P}(\Delta t) = I + \bar{A}(\phi)\Delta t + O(\Delta t^2)$. Substituting $P(\Delta t)$ and $\bar{P}(\Delta t)$ into (7), for $k,l\in\bar{\mathcal{V}}$, we have

$$\begin{aligned} &\mathbb{1}_{\{k=l\}} + \bar{A}_{kl}(\phi)\Delta t + O(\Delta t^2) \\ &= \frac{\sum_{i\in\phi^{-1}(k)}\sum_{j\in\phi^{-1}(l)}\pi_i(\mathbb{1}_{\{i=j\}} + A_{ij}\Delta t + O(\Delta t^2))}{\sum_{i\in\phi^{-1}(k)}\pi_i} \\ &= \mathbb{1}_{\{k=l\}} + \frac{\sum_{i\in\phi^{-1}(k)}\sum_{j\in\phi^{-1}(l)}\pi_i A_{ij}}{\sum_{i\in\phi^{-1}(k)}\pi_i}\Delta t + O(\Delta t^2). \end{aligned}$$

By matching terms on both sides of above equation, we obtain the formula for the optimal super-transition-rate matrix

$$\bar{A}_{kl}(\phi) = \frac{\sum_{i\in\phi^{-1}(k)}\sum_{j\in\phi^{-1}(l)}\pi_i A_{ij}}{\sum_{i\in\phi^{-1}(k)}\pi_i}, \quad k,l\in\bar{\mathcal{V}}. \quad (10)$$

By substituting (2) and (4) into (10), we can express $\bar{A}$ as:

$$\bar{A}_{kl}(\phi) = \begin{cases} \dfrac{\sum_{i\in\phi^{-1}(k)}\sum_{j\in\phi^{-1}(l)} 1/R_{ij}}{\sum_{i\in\phi^{-1}(k)} C_i}, & k\neq l \\ -\displaystyle\sum_{\tilde{k}\neq k} \bar{A}_{k\tilde{k}}(\phi), & k = l \end{cases} \qquad (11)$$

The transition rate matrix structure of $\bar{A}$ implies that we can also define super-quantities to form a RC-network. For the kth super-node, by substituting (4) into (8), we obtain the optimal stationary distribution:

$$\bar{\pi}_k(\phi) = \sum_{i\in\phi^{-1}(k)}\pi_i = \frac{\sum_{i\in\phi^{-1}(k)} C_i}{\sum_{l\in\bar{\mathcal{V}}}\sum_{j\in\phi^{-1}(l)} C_j}. \qquad (12)$$

Recall that the stationary distribution of the aggregated Markov chain can also be represented as (see (4)):

$$\bar{\pi}_k(\phi) = \frac{\bar{C}_k(\phi)}{\sum_{l\in\bar{\mathcal{V}}}\bar{C}_l(\phi)} \qquad (13)$$

where $\bar{C}_k(\phi)$ denotes the *super-capacitance* for the kth super-node. By comparing (12) and (13), we obtain:

$$\bar{C}_k(\phi) = \sum_{i \in \phi^{-1}(k)} C_i. \tag{14}$$

By using (11) and (14), we obtain the formula for the *super-resistance* for any two adjacent super-nodes k and l:

$$\bar{R}_{kl}(\phi) = \frac{1}{\bar{C}_k(\phi)\bar{A}_{kl}(\phi)} = \frac{1}{\sum_{i \in \phi^{-1}(k)} \sum_{j \in \phi^{-1}(l)} 1/R_{ij}}.$$

The above well-defined super-quantities provide an intuitive justification of the aggregation approach. The reduced-order linear model (5) corresponds to a reduced RC-network with super-capacitances and super-resistances given above.

Consider a scalar-valued function $\bar{V}(t) := \sum_{k \in \bar{\mathcal{V}}} \bar{C}_k(\phi)\bar{T}_k(t)$. One can verify that $\bar{V}(t) = \bar{V}(0)$ for all $t \geq 0$ due to the RC-network structure of the reduced linear model. Choose the initial condition for the reduced-order model (5) as $\bar{T}_k(0) = \sum_{i \in \phi^{-1}(k)} (C_i/\bar{C}_k(\phi)) T_i(0)$ for $k \in \bar{\mathcal{V}}$, then

$$\bar{V}(0) = \sum_{k \in \bar{\mathcal{V}}} \sum_{i \in \phi^{-1}(k)} C_i T_i(0) = \sum_{i \in \mathcal{V}} C_i T_i(0) = V(0).$$

This implies that the invariant quantity of the linear thermal dynamics is unchanged after the aggregation. Thus, we can define an aggregated probability distribution:

$$\bar{f}_k = \frac{\bar{C}_k}{\bar{V}(0)} \bar{T}_k, \quad k \in \bar{\mathcal{V}}. \tag{15}$$

Using the lifting technique similar to (6), we define a lifted probability distribution

$$\widehat{f}_i = \frac{\pi_i}{\sum_{j \in \psi(i)} \pi_j} \bar{f}_{\phi(i)}, \quad i \in \mathcal{V}. \tag{16}$$

Let $\widehat{T}$ denote the lifted temperature on the original state space $\mathcal{V}$. The lifted distribution can also be expressed as

$$\widehat{f}_i = \frac{C_i}{V(0)} \widehat{T}_i, \quad i \in \mathcal{V}. \tag{17}$$

Substituting (4) and (15) into (16), we have

$$\widehat{f}_i = \frac{C_i}{\sum_{j \in \psi(i)} C_j} \frac{\bar{C}_{\phi(i)}}{\bar{V}(0)} \bar{T}_{\phi(i)} = \frac{C_i}{V(0)} \bar{T}_{\phi(i)} \tag{18}$$

where we use the fact that $\bar{C}_{\phi(i)} = \sum_{j \in \psi(i)} C_j$ and $\bar{V}(0) = V(0)$. By comparing (17) and (18), we have the explicit expression for the lifted temperature

$$\widehat{T}_i = \bar{T}_{\phi(i)}, \quad i \in \mathcal{V}.$$

Thus, we can compare the full and reduced-order models by directly comparing T_i and $\bar{T}_{\phi(i)}$ for each node i.

3.5 Reduced nonlinear building thermal model

In this section, we aggregate the nonlinear part of building thermal model using the same partition function obtained from the analysis of the linear thermal dynamics. Due to the current source interpretation of nonlinear term $L(T, U, \dot{Q})$ (see Remark 1), the current sources connecting to the same super-nodes are directly added up to form a super-current source for the corresponding super-node:

- For $k = 1, \ldots, m$, the aggregated nonlinear part thermal dynamics is given by:

$$\begin{aligned} \widetilde{L}_k(T, U, \dot{Q}) &= \sum_{i \in \phi^{-1}(k)} C_i L_i(T, U, Q)/\bar{C}_k(\phi) \\ &= (C_{pa}(T^s \bar{U}_k(\phi) - \widetilde{W}_k(\phi)) + \dot{\bar{Q}}_k(\phi))/\bar{C}_k(\phi) \end{aligned} \tag{19}$$

  where $\bar{U}_k(\phi) := \sum_{i \in \phi^{-1}(k)} U_i$, $\dot{\bar{Q}}_k(\phi) := \sum_{i \in \phi^{-1}(k)} \dot{Q}_i$, and $\widetilde{W}_k(\phi) := \sum_{i \in \phi^{-1}(k)} U_i T_i$.
- For $k = m+1$, the aggregated nonlinear thermal dynamics is given by:

$$\widetilde{L}_{m+1}(T, U, \dot{Q}) = \eta.$$

  The construction here is to make sure $\bar{T}_{m+1}(t) = T_o(t)$ in the reduced-order model (21) described later.

Since U and Q are external inputs to the full-order model, we can also take $\bar{U}(\phi)$ and $\dot{\bar{Q}}(\phi)$ as the *super-inputs* to the reduced-order model. One problem is that the term $\widetilde{W}(\phi)$ depends on T, which is the state vector of the full-order model. We use $\bar{T}_k$ to approximate the T_i that belongs to the same kth group, and obtain an approximation to $\widetilde{W}_k(\phi)$:

$$\bar{W}_k(\phi) := \sum_{i \in \phi^{-1}(k)} U_i \bar{T}_k = \bar{U}_k(\phi)\bar{T}_k, \quad k = 1, \ldots, m.$$

Replacing $\widetilde{W}_k(\phi)$ by $\bar{W}_k(\phi)$ in (19), we can approximate $\widetilde{L}_k(T, U, \dot{Q})$ by

$$\begin{aligned} &\bar{L}_k(\bar{T}, \bar{U}(\phi), \dot{\bar{Q}}(\phi)) \\ &\qquad = \left(C_{pa}\bar{U}_k(\phi)(T^s - \bar{T}_k) + \dot{\bar{Q}}_k(\phi)\right)/\bar{C}_k(\phi) \end{aligned} \tag{20}$$

for $k = 1, \ldots, m$ and $\bar{L}_{m+1}(\bar{T}, \bar{U}(\phi), \dot{\bar{Q}}(\phi)) = \eta$. By combining the aggregated linear dynamics (5) with the aggregated nonlinear dynamics (20), we obtain the reduced-order building thermal model:

$$\frac{d\bar{T}}{dt} = \bar{A}(\phi)\bar{T} + \bar{L}(\bar{T}, \bar{U}(\phi), \dot{\bar{Q}}(\phi)). \tag{21}$$

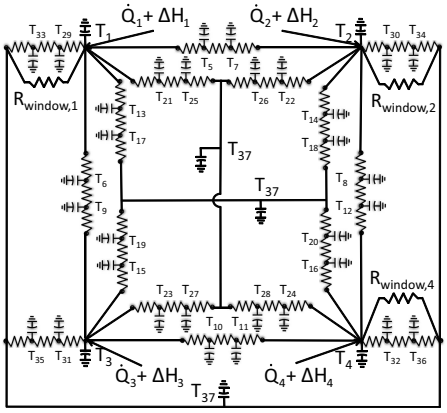

Fig. 2. RC-network representation of the four-zone building shown in Fig. 1, where $\dot{Q}_i$ and $\Delta H_i = C_{pa} U_i (T^s - T_i)$ denote the total heat gain and heat exchange for the ith zone, respectively.

Remark 2 Similar to the full model (1), the reduced model (21) also corresponds to a RC-network defined with super-nodes and super-edges. The linear term $\bar{A}(\phi)\bar{T}$ captures the aggregated thermal interactions of the neighboring super-nodes, and the nonlinear term $\bar{L}(\bar{T}, \bar{U}(\phi), \dot{\bar{Q}}(\phi))$ can be interpreted as the aggregated current sources connecting to the super-nodes. Thus, the model reduction method proposed in this paper preserves the RC-network structure of the building thermal model.

Remark 3 The reduced-order model so far depends on the choice of the partition function ϕ. The optimal partition function ϕ^* can be obtained by applying the recursive bi-partition algorithm to Markov chain corresponding to the linear thermal dynamics. We should also mention that, in practice, one can also directly choose a sub-optimal ϕ^* based on physical intuition (e.g., floor plans in a multi-zone building), or some other kinds of expert-based heuristics.

4 Simulation and Discussion

In this section, we consider the four-zone building shown in Fig. 1 to demonstrate the aggregation-based model reduction method proposed in this paper. Each of the four zones/rooms has an equal floor area of $5\mathrm{m} \times 5\mathrm{m}$ and each wall is $3\mathrm{m}$ tall. Room 1 has a small window ($5\mathrm{m}^2$) on the north facing wall, whereas rooms 2 and 4 have larger windows ($7\mathrm{m}^2$ each) on the east facing wall. Room 3 does not have a window. The supply air temperature of the HVAC system is fixed at $T^s = 12.8°\mathrm{C}$. The maximum supply air mass flow rate for each room is $0.25\mathrm{kg/s}$. The outside temperature T_o and heat gains $\dot{Q}$ are taken as the same as those used in our previous work (see Figure 2 in [5]). All temperatures are initialized at $24°\mathrm{C}$. The time step size is chosen as $\Delta t = 10$ minutes and the total simulation time is 24 hours.

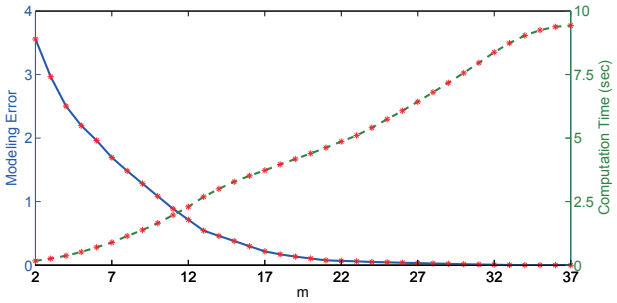

Fig. 3. Modeling error and computation time for aggregating the linear thermal dynamics with respect to the number of partitions.

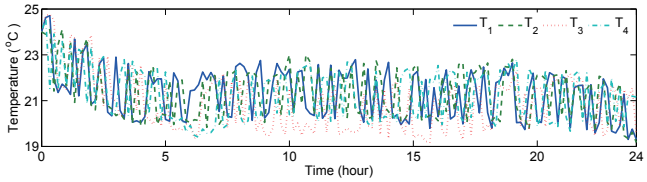

Fig. 4. Four zone temperatures $T_1, \ldots, T_4$ simulated by the full 36th-order model.

4.1 *Recursive bi-partition of building graph*

The RC-network representation of the four-zone building model is shown in Fig. 2. There are total 36 building nodes plus 1 outside node: 4 zone nodes $\{1, \ldots, 4\}$, 8 internal-wall nodes $\{5, \ldots, 12\}$, 8 internal-floor nodes $\{13, \ldots, 20\}$, 8 internal-ceiling nodes $\{21, \ldots, 28\}$, 8 external wall nodes $\{29, \ldots, 36\}$, and 1 outside node $\{37\}$. The values of thermal resistances and thermal capacitances are obtained from Carrier Hourly Analysis Program [1]. The outside node is assumed to have a very large capacitance $C_{37} = 10^{10}\mathrm{KJ}/(\mathrm{m}^2\mathrm{K})$ for constructing the Markov chain.

The recursive bi-partition algorithm, described in Section 3.3, is used to find multiple partitions of the building graph based on the analysis of the linear thermal dynamics. For example, for the 5-partition, the algorithm returns five groups of nodes with clear physical intuition: group i contains all nodes connected to room i, for $i = 1, \ldots, 4$, and group 5 consists of the single outside node $\{37\}$. More detailed partition results were reported in our previous work [6]. In Fig. 3, we plot the modeling error in terms of KL divergence rate with respect to the number of partitions. Note that the m-partition corresponds to the $(m-1)$ super-nodes and 1 outside node. In Fig. 3, we also plot the computation time for obtaining each partition function through the recursive bi-partition algorithm. We observe that the modeling error monotonically decreases and computation time monotonically increases as the number of partitions increases. The modeling error plot in Fig. 3 will also be used in the next section as a conservative guideline for the model reduction of the nonlinear model.

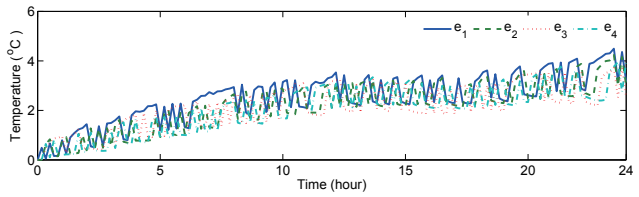

Fig. 5. Simulation comparison of nonlinear building thermal model with its linearized model. The simulation errors are given by $e_i = \widetilde{T}_i - T_i$ for $i = 1, \ldots, 4$, where T_i is the temperature simulated by the full-order nonlinear model and $\widetilde{T}_i$ is the temperature simulated by the linearized model.

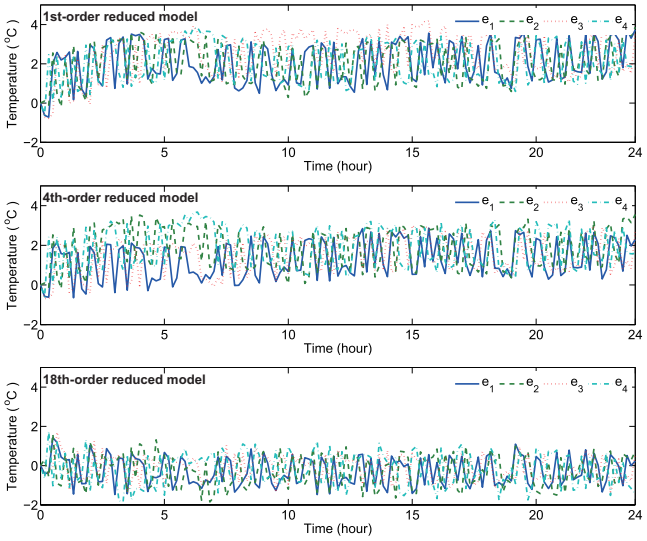

Fig. 6. Four zone temperature simulation errors are given by $e_i = \widehat{T}_i - T_i$ for $i = 1, \ldots, 4$, where T_i is the temperature simulated by the full-order model and $\widehat{T}_i$ is the lifted temperature simulated by the 1st-order, 4th-order, and 18th-order reduced models.

4.2 Simulation of reduced-order models

The full-order model (1) is used to represent the full building thermal dynamics, with 36 building nodes plus 1 outside node. The partition functions obtained in Section 4.1 are used to construct the reduced-order model (21). All simulations reported here are open-loop simulations with mass flow rates $\dot{m}_i^{in}$ for $i = 1, \ldots, 4$ taken as random binary signals in the range of 0kg/sec to 0.25kg/sec. The Matlab function idinput is used to generate the required random binary signals. To test the goodness of the reduced-order models, we compare the four zone temperatures simulated by the full and reduced-order models. When simulated by the full-order model, the temperature of room i is denoted by T_i. When simulated by the reduced-order model, the lifted temperature of room i is denoted by $\widehat{T}_i$. The ith zone temperature simulation error is given by $e_i(j\Delta t) = \widehat{T}_i(j\Delta t) - T_i(j\Delta t)$ for $j = 0, \ldots, N_s$, where $N_s = 144$ here.

All simulations reported here are implemented in Matlab using the fourth-order Runge-Kutta method with a fixed time step $\Delta t = 10$ minutes. Note that Δt is chosen as the same for both full and reduced-order models for a fair comparison of the their simulation times. We run 20 independent simulations for assessing all kth-order reduced models for $k = 1, \ldots, 36$. Note that the kth-order reduced model corresponds to the $(k+1)$-partition described in Section 4.1 with k super-building nodes and 1 outside node. For each run of simulation, we independently generate the random binary signals as inputs and all reduced-order models are simulated with the same generated inputs. Taking one run for example, Fig. 4 shows the temperatures of the four zones simulated by the full 36th-order nonlinear building thermal model. Fig. 5 compares the simulation results of the full 36th-order model and its linearized model. The system linearization point is taken as the initial condition of the nonlinear model. We observe that the performance of the linearized model is degraded as the actual operation points move away from the vicinity of system linearization point. Fig. 6 shows the temperature simulation errors corresponding to reduced-order models with varying degree of reduction: (i) 1st-order reduced model (1 super-node representing all building nodes), (ii) 4th-order reduced model (4 super-nodes representing 4 groups of nodes associated with 4 zones), and (iii) 18th-order reduced model. We observe from Fig. 6 that, as expected, simulation errors decrease as the order of the reduced model increases. For the 18th-order model, the simulation error for all four zones are all between the range of $-2°\text{C}$ to $2°\text{C}$. Note that even in a building that meets ASHRAE thermal comfort standards, the temperature inside a zone may vary by up to $3°\text{C}$ [2].

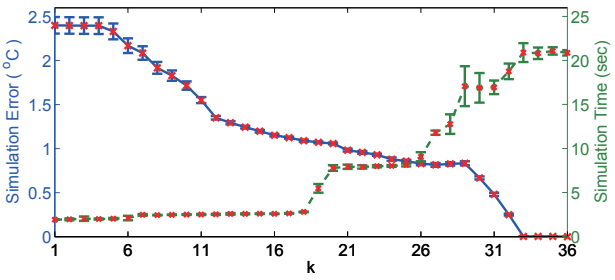

Fig. 7. Simulation error and simulation time for the kth-order reduced model. The error-bar plot depicts the mean and standard deviation of the curve for 20 independent runs.

For each run of simulation, the simulation error for the kth-order model is defined as a root mean squared error averaged over four zones:

$$\text{Err}_k := \frac{1}{4}\sum_{i=1}^{4}\sqrt{\frac{\sum_{j=0}^{N_s}(\widehat{T}_i(j\Delta t) - T_i(j\Delta t))^2}{N_s+1}}.$$

In Fig. 7, we depict the error-bar plot of the simulation errors for 20 independent runs, where error bars quantify the deviations of different simulation runs. In Fig. 7, we also depict the error-bar plot of the simulation times for running Matlab simulations with different reduced-order models. For different degree of reduction, the total computational com-

plexity can be evaluated by summing up the computation time in Fig. 3 to the simulation time in Fig. 7. As expected, we observe from Fig. 7 that the simulation error decreases while simulation time increases as the order of the reduced model increases. We also observe from Fig. 7 that the simulation error decreases quickly and simulation time increases slowly when model order is less than 18. For the 18th-order model, the simulation error drops down to an acceptable level, and the simulation time still maintains in the same level as compared to those lower-order models. Thus, one may take 18th-order model as a good candidate to approximate the full-order model with acceptable simulation error and much lower simulation time. In practice, one can make a tradeoff between the simulation accuracy and computational complexity of the reduced order model by choosing an appropriate order of reduction.

4.3 Discussion

First of all, the open loop tests considered in this paper may not be sufficient for assessing the proposed model reduction method. More open loop assessments with random inputs need to be considered to fully excite nonlinear building dynamics. More closed loop assessments with various building control profiles also need to be considered for practical implementation in real buildings. On the other hand, the full-order model considered here does not have inter-zone convection effects that is difficult to model due to the complex physics that govern this phenomena. Recently, a data-driven identification scheme was proposed to obtain a RC-network model of convection among zones [16]. The aggregation-based method is immediately applicable if the full-order model is augmented by such convection models.

In current work, the model reduction method needs to start from a fully parameterized baseline model. The reduced-order models are then obtained by analyzing the baseline model. In future, we plan to apply the learning-based approaches [7], which only require locally exploiting the building graph through simulations, to search for the optimal coordination of aggregation. We are also developing decentralized optimal control strategies for energy-efficient buildings based on the aggregated building model. The main idea is to use aggregated models to capture the mean field or net effect of the entire building envelope on any individual zone. Then an optimal control law for each zone is developed as a function of local zone temperature and mean field information captured by the aggregated model. See [5] for more details.

5 Conclusions

We proposed a method to reduce the order of a multi-zone building thermal model via aggregation of states. We first establish a Markov chain analogy to the linear part of the building model. A recently developed Markov aggregation method is then applied to obtain the optimal aggregation of the state space. Extension of the aggregation method to the nonlinear part of the model is carried out by aggregating inputs accordingly into the super-inputs. A key advantage of the proposed method is that the reduced model is still a RC-network model with the same structure as the original model but with less number of nodes and less parametric information. This makes the reduced model useful not only for simulation and analysis but also for building design iterations.

References

[1] *HAP Quick Reference Guide*. Carrier Corporation, Farmington, CT, 2003.

[2] American Society of Heating, Refrigerating and Air-Conditioning Engineerrs, Inc. ANSI/ASHRAE standard 55-2004, thermal environmental conditions for human occupancy, 2004.

[3] A. Aswani, N. Master, J. Taneja, V. Smith, A. Krioukov, D. Culler, and C. Tomlin. Identifying models of HVAC systems using semiparametric regression. In *Proceedings of American Control Conference*, pages 3675–3680, Montréal, Canada, 2012.

[4] J. E. Braun and N. Chaturvedi. An inverse gray-box model for transient building load prediction. *HVAC&R Research*, 8(1):73–99, 2002.

[5] K. Deng, P. Barooah, and P. G. Mehta. Mean-field control for energy efficient buildings. In *Proceedings of American Control Conference*, pages 3044–3049, Montréal, Canada, 2012.

[6] K. Deng, P. Barooah, P. G. Mehta, and S. Meyn. Building thermal model reduction via aggregation of states. In *Proceedings of American Control Conference*, pages 5118–5123, Baltimore, MD, 2010.

[7] K. Deng, P. G. Mehta, and S. P. Meyn. A simulation-based method for aggregating Markov chains. In *Proceedings of IEEE Conference of Decision and Control*, pages 4710–4716, Shanghai, China, 2009.

[8] K. Deng, P. G. Mehta, and S. P. Meyn. Optimal Kullback-Leibler aggregation via the spectral theory of Markov chains. *IEEE Trans. Automat. Contr.*, 56(12):2793–2808, 2011.

[9] J. R. Dobbs and B. M. Hencey. A comparison of thermal zone aggregation methods. In *IEEE Conference on Decision and Control*, pages 6938–6944, Maui, Hawaii, USA, 2012.

[10] EnergyPlus. www.eere.energy.gov/buildings/energyplus. U.S. Department of Energy (DOE).

[11] A. Foucquier, S. Robert, F. Suard, L. Stephan, and A. Jay. State of the art in building modelling and energy performances prediction: A review. *Renewable and Sustainable Energy Reviews*, 23:272–288, 2013.

[12] M. Georgescu, B. Eisenhower, and I. Mezic. Creating zoning approximations to building energy models using the Koopman operator. In *Proceedings of IBPSA-USA's SimBuild 2012 Conference*, Madison, Wisconsin, 2012.

[13] M. M. Gouda, S. Danaher, and C.P. Underwood. Building thermal model reduction using nonlinear constrained optimization. *Building and Environment*, 37(12):1255–1265, 2002.

[14] S. Goyal and P. Barooah. A method for model-reduction of nonlinear building thermal dynamics. *Energy and Buildings*, 47:332–340, April 2012.

[15] S. Goyal, H. Ingley, and P. Barooah. Zone-level control algorithms based on occupancy information for energy efficient buildings. In *Proceedings of American Control Conference*, pages 3063–3068, Montréal, Canada, 2012.

[16] S. Goyal, C. Liao, and P. Barooah. Identification of multi-zone building thermal interaction model from data. In *50th IEEE Conference on Decision and Control and European Control Conference*, pages 181–186, December 2011.

[17] J. Hahn and T. F. Edgar. An improved method for nonlinear model reduction using balancing of empirical gramians. *Computers & Chemical Engineering*, 26(10):1379–1397, 2002.

[18] S. A. Klein. *A Transient System Simulation Program*. Solar Energy Laboratory, Madison, WI, 1996.

[19] S. Lall, J. E. Marsden, and S. Glavaski. A subspace approach to balanced truncation for model reduction of nonlinear control systems. *International Journal of Robust and Nonlinear Control*, 12(6):519–535, 2002.

[20] Y. Ma, G. Anderson, and F. Borrelli. A distributed predictive control approach to building temperature regulation. In *Proceedings of American Control Conference*, pages 2089–2094, San Francisco, CA, 2011.

[21] M. Maasoumy and A. Sangiovanni-Vincentelli. Total and peak energy consumption minimization of building HVAC systems using model predictive control. *Design & Test of Computers, IEEE*, 29(4):26–35, 2012.

[22] J. Scherpen. Balancing for nonlinear systems. *Systems & Control Letters*, 21(2):143–153, 1993.

[23] D. W. Stroock. *An Introduction to Markov Processes*. Springer, New York, NY, 2005. Volume 230 of Graduate texts in mathematics.

[24] Y. Yu. *Model-Based Multivariate Control of Conditioning Systems for Office Buildings*. PhD thesis, Carnegie Mellon University, 2012.

[25] M. Zaheeruddin and G. R. Zheng. Optimal control of time-scheduled heating, ventilating and air conditioning processes in buildings. *Energy Conversion and Management*, 41(1):49–60, 2000.